International Journal of Engineering Trends and Technology
ISSN: 2231 – 5381 /doi:10.14445/22315381/IJETT-V69I7P222
Volume 69 Issue 7, 159-166, July, 2021

Medical Diagnosis Model based on Spiking Neural Network considering Normalization of Histogram and Wavelet Transform Features of Medical Images

Ashish Kumar Dehariya[#1], Pragya Shukla[*2]

[1]*Dept of Computer Engineering, IET, DAVV, Indore, India*
[2]*Dept of Computer Engineering, IET, DAVV, Indore, India*

[1]ashish.mehra3@gmail.com

Abstract *- Experts diagnose most diseases by interpreting medical images. The same task can be performed with improved accuracy by automating medical diagnosis algorithms. Convolutional Neural Network (CNN) classifies medical images considering continuous features. Sometimes processing of unnecessary features increases computation time also decreases classification accuracy. This research processed extracted medical image features by Spiking Neural Network(SNN). SNN uses time-based input spikes and overlooks the processing of useless input features hence obtain improved classification accuracy. Second level discrete wavelet transform and histogram features utilized in the proposed approach to prepare a normalized vector for the training of spiking neural network. The experiment was done on real medical image datasets. For each 125 image dataset Spiking Neural Based Medical Image Diagnosis (SNMID) gives an accuracy percentage of 91.20 for malaria, 87.67 for breast cancer, and 100 for skin cancer, whereas CNN based medical image diagnosis(CNMID) lacks the accuracy having measures 57.72 for malaria, 78.05 for breast cancer, 69.12 for skin cancer. Precision, recall, and f-measure values also found improved in the case of SNMID.*

Keywords — *Convolutional Neural Network, Discrete Wavelet Transform, Histogram Features, Medical Image Diagnosis, Spiking Neural Network.*

I. INTRODUCTION

In the proposed model, Spiking Neural Based Medical Image Diagnosis(SNMID) works for finding the classes (Normal / Infected or Benign/Malignant) of medical images belongs to malaria, breast cancer, and skin cancer datasets. The artificially intelligent system incorporates medical industries for early diagnosis of the patient's disease[1]. As per the medical reports of a patient, experts diagnose disease. High-quality images are usually get generated by various techniques like X-Ray, CT-Scan, MRI, etc. [2]. It increases the dependency of a radiologist, pathologist to detect symptoms for such images. Diseases diagnosis depends on the test reports, and technology increases the easiness with high accuracy and justifies precision output. Most of the computer vision algorithms were developed to identify the image content and classify images as per visual information reflected by X-Ray, Light, Magnet, etc. [3]. Still, the classification of medical images into correct classes for different diseases is a major issue to solve.

In order to strengthen the medical diagnosis, learning models were proposed by researchers. Image features get extracted from the reports for classification. Various visual contents such as edges, histogram, DWT, DCT, etc. [4] were used in work. Extracted features get trained in different learning models named CNN, RNN, DNN, etc. [5]. Most of the models proposed earlier were tested on a single image medical dataset. One multi-disease diagnosis system saves cost and time. Our work also concentrated on multi diseases diagnosis with high accuracy output. This research work has the following set of objectives.

1. Extract light and effective features from the medical images.
2. Normalize various feature set values into a single domain as each feature has different ranges.
3. Train a machine learning model to identify the feature class as per desired output.

The Paper is structured into few sections. The first is an introduction, and the second section gives a brief overview of various soft computing approaches that have already been adopted by different authors to detect malaria, breast cancer, and skin cancer. Further proposed methodology, i.e., SNMID is described, which included a detailed explanation by flow chart and algorithm. The experiment and result section shows the comparison of the proposed methodology with existing work that is based on CNN-based medical image diagnosis. Finally, work gets concluded with future prospects.

II. LITERATURE SURVEY

Mehedi Masud et al. in [6] proposed an algorithm that identified malaria symptoms and gave mobile healthcare solution. Authors proved deep learning architecture to be useful in detecting malaria disease in real-time accurately by inputting images and thus reduces the manual labor in the detection of the disease. By solving the data overfitting issue, this model performance can be improved.

Fuhad et al. in [7] proposed a deep learning technique by which analysis can be done automatically. The need for trained professionals drastically reduced as the model gives accurate and automatic results. This model was based on Convolutional Neural Network and can be used in the diagnosis of malaria by taking input in the form of microscopic blood smear images. Here techniques included autoencoder, knowledge distillation, and data augmentated features and classified using forms of k-nearest neighbors or support vector machine. Three training procedures, namely autoencoder, general distillation, and distillation training, were used to improve the accuracy of the model. Here too many complex computations were involved behind result outcomes.

P. A. Pattanaik et al. in [8] given a comprehensive CAD concept for identifying the parasites of malaria in the blood smear images. The parameters of this model got trained by using soft computing techniques followed by a stacked autoencoder. 12500-2500-100-50-2 were the various optimum size that kept for this CAD scheme, out of which the input layer consist of 12500 nodes and the output layer of the softmax classifier possessed 2 nodes. A 10 fold cross-validation system was used to prove the reliability of this model by comparing it with blood smear images of new patients however processed continuous input features lack the accuracy performance.

Sahni P. et al. in [9] given an MRI and a mammogram as the two important modalities to detect accurately the portions of the body that contains tumors. The tumourous part of the body was then separated from the extracted image by using the segmentation method together with the threshold model and edge detection method. Here Edge detection method produced a better result than the threshold-based model; however it suffers noise-sensitive issues also on the smooth transition of an image, proper working was not justified.

Y. Wang et al. in [10] proposed an automatic ultrasound for the breast region. The method was found to be more innovative and promising for screening the breast region. As compared to the conventional B-mode, 2-dimensional ultrasound, the ABUS is operator-free and provides a 3D image of the whole breast. But the reviewing of the obtained ABUS images is time-intensive, and oversight errors may occur. To solve this issue, a new 3D CNN network was introduced to be incorporated in ABUS so that reviewing can be accelerated to achieve a high level of sensitivity together with low false positives. The paper had given a deep method of supervision to increase the sensitivity by using the multi-layer features. This paper also calculated a threshold loss for the voxel level for finding out the difference between cancer and non-cancer regions to attain higher sensitivity together with low false positives conditions. Here 3D CNN also considers an image having some noise, and then it considered the same as a completely different image; hence performance degradation occurs.

J. Zheng et al. in [11] proposed the work started with an examination of breast masses for several diagnostics by using a CNN-based transfer process. It included prognostic and predictive tasks in several image patterns such as mammography, digital breast tomosynthesis, and MRI of magnetic resonance imaging. The layer contains many convolutional layers, Max-pooling, and LSTM layers. The classification was also performed in the softmax layer and fully connected layer. The paper focused on the concept of combining such machine learning concepts for finding out the desired features and extracting them by recognizing and using this data for evaluating their output by segmentation and various other techniques for accurate results.

Shivangi Jain et al. in [12] given a method for the detection of skin cancer named Melanoma by using a computer-aided method and various image processing tools. At first, the input to this system was given in the form of a skin lesion image, and then it is passed through unique image processing techniques to analyze the possibility of cancer in the sample. The image analysis tools checked for various Melanoma cancerous conditions parameters such as ABCD, diameter, asymmetry, border colors by analyzing the shape, size, and texture of the sample and segmenting them in various stages.

Kalwa, U. et al. in [13] presented a smartphone app to capture the border irregularity, asymmetry, color variegation, and diameter of the entered skin lesion sample. Using all the above features, the classification of the malignancy was provided by using concept vector machine classifiers. Several adaptive algorithms and data processing algorithms were used to make the app user-friendly and reliable to detect Melanoma cancerous conditions in the skin lesion. Input can be in the form of public datasets or images captured from the camera. The app runs on any android smartphone that is equipped with a detachable lens of 10x and can process the image in a second.

Mohammad Ashraf Ottom in [14] built a deep learning computer model to predict the cases of cancer. The first stage was to analyze the image and segment and prepare its data to find the useful part of an image. It also reduces the amount of noise and illumination in images to detect the sharp boundaries of the image. Finally, the proposed scheme of the network contains three max-pooling layers, three convolution layers together with four fully connected layers.

Divya Srivastava et al. [15] reviewed that local and global correlogram and histogram can be used to extract color features of an image. An image can be represented using its

shape, involved color level, and texture features. Histogram features of an image show the frequency separations of colors hence treated as the considerable agent to deal with while image processing. Haar wavelet works in RGB color space to extract image features[16]. From four of the decomposed components, the approximation component contains the required features to represent an image.

Naoya Muramatsu at al.[17] stated the difference between artificial neural network(ANN)/ CNN and Spiking Neural Network. ANN/CNN is used to process continuous inputs, whereas SNN handles discrete time-based input features. Taeyoon Kim et al.[18], declared that SNN involves fewer computations during processing. It simulates the signal processing behavior of biological neural networks[19]. For pattern recognition, SNN gives a fast and efficient performance in evaluating results[20]. Presynaptic and postsynaptic mechanism initially decides weights for neurons[21]. In a network, one neuron passes the information to the next neuron only when the threshold value is reached. After firing some set of information, involved neurons state set to null hence less important features avoided during computations causing SNN found a better approach to work with and for achieving improved accuracy level.

III. PROPOSED MODEL

In the proposed model, extracted and normalized input features get passed through a spiking neural network for classification; hence Spiking Neural Based Medical Image Diagnosis (SNMID) name is given. In SNN, input features are considered as a set of time-based spikes. These spikes get accumulated in the processing unit of neurons, then collected pieces of information passed through neurons only when threshold level get reached. Proposed SNMID work was divided into two modules first was the training of neural networks by extracted image features sets, and the other was the testing of trained neural networks. The whole working steps for training the proposed model are shown in Fig. 1 while spiking neural multilayer connections are shown in Fig.2. Various annotations used in work are detailed in table 1.

A. Pre Processing

Input image dataset needs to be preprocessed firstly as training dataset should be of same dimension and format.

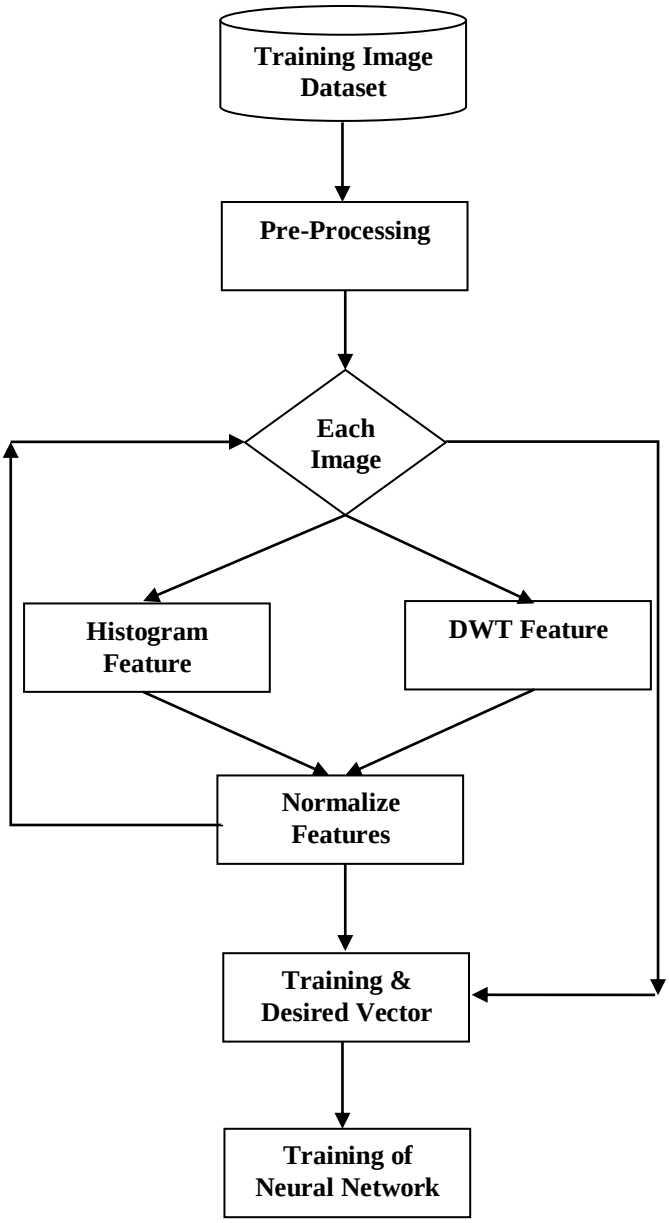

Fig: 1 Training of proposed model.

As the training dataset has labeled images either infected/malignant or normal/benign hence image labels were stored in separate desired vector D. In this step of the proposed model, the dimension of each image was resized into a fixed mxn matrix. All input images were transformed into the gray format. To increase the work efficiency input image, I got blocked into bxb size. So the image has a B number of blocks.

$$B = (mxn)/(bxb) \quad \text{Eq.1}$$

Each block was treated separately for feature extraction and training of neural networks in the model. D vector for

each block of the same image has 0 or 1 value where 0 is for normal/benign, and 1 is for infected/malignant condition.

TABLE 1. LIST OF ANNOTATION

Annotation	Meaning
I	Input Image
m,n	Image dimension
D	Desired Vector
b	Block size
H	Histogram Feature matrix
DWT	DWT Feature Matrix
N	Normalize Vector
P	Post / Pre Synapses
w	Weight between Layer
E	Error
T_{NN}	Trained Neural Network

B. Histogram Features

The blocked image was processed further for getting the image histogram feature having a p number of bins. This p can be either {8, 16, 32,..256} range. This can be understood if p=8, then image values were divided into 8 bins [22]. So for gray image pixels value ranged from 0 to 255 then 8 bins are from [{0-31}, {32-63}, {64-95}, …….{233-255}]. So the output of the histogram feature was a vector having p elements, count of blocks for each bin that pixels present. The Sum of the p vector is equal to bxb cells. In Eq.2, $H_{i,B}$ is a matrix of p number of columns and B number of rows for the i^{th} image.

$$H_{i,B} = \text{Histogram}(B, p) \qquad \text{Eq.2}$$

C. DWT Features

The blocked image was processed further to get the DWT feature from the block of the bxb dimension [23]. Input block was transformed into frequency domain having four submatrix of b/2xb/2 dimension. The proposed model utilized all sets of transforming the frequency-domain value of block as a DWT feature in work.

D. Normalize Features

The feature set obtained from a histogram as a vector and DWT as a matrix have different coefficient ranges. So, first of all, prepared a single vector N of both features with a total p+B number of elements. For each block normalized feature vector was prepared as per spike data of 0 / 1. Each element in the N vector having a non-zero value was set as 1. Elements with value 1 acted as the spike in the N vector, and others acted as the dead coefficient value in the signal.

E. Training Vector

The normalized vector obtained from the above step was combined with other desired output vectors of block D. Tv is a vector having [N, D] values obtained from the above steps. In training, both N and D were passed, while in testing, only N was passed.

F. Training of Spiking Neural Network

a) Initialization of Pre and Post Synaptic of SNN:

In a genetic neural network, each neuron communicates with other neurons by a synapses junction. So input signal passes through pre synapses and post synapses portion. This transition of the signal makes a change in signal values [24, 25]. In order to reflect such a process in the artificial spiking neural network, Eq. 3 shows the signal changes.

$$P_{rs}(t) = \int_0^N K_{syn}(t - t^f) e^{\frac{-t}{\tau}} \qquad \text{Eq. 3}$$

K_{syn} is a constant that controls conductance peak value in the network. The time constant of the synaptic was represented byτand t is a time interval when fire occurs in the network. Normally N represents the signal vector element count.

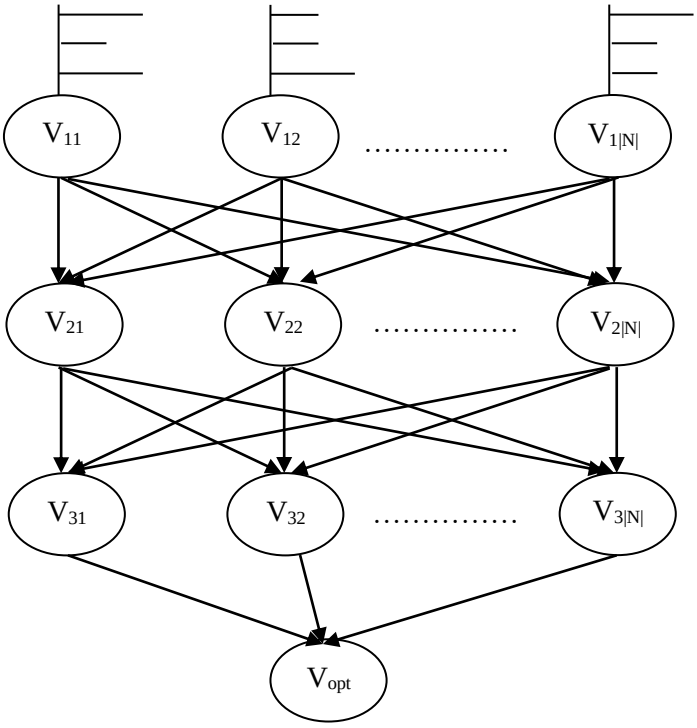

Fig: 2 Spiking neural network multilayer connection.

In a similar fashion, post synapses values were formulated by Eq. 4. Here V(t) denotes the membrane potential of a neuron.

$$P_{os}(t) = \int_0^\infty P_{os}(t) - V(t) \int_0^\infty P_{os}(t) \qquad \text{Eq. 4}$$

In order to get the initial weight value of the spiking neural network, Eq. 5 is included.

b) Weight, output, error calculation, and adjustment:

$$w_{ij}(t) = a_o + a_1 P_{rs}(t) + a_2 P_{os}(t) + a_3 P_{rs}(t) P_{os}(t) + a_4 P_{rs}(t) P_{os}(t) \qquad \text{Eq. 5}$$

As shown in Fig. 2, nodes acted as the artificial neurons, and the connecting edge between nodes acted as synaptic. In above Eq. 5, $w_{ij}(t)$ is the weight between the i^{th} and j^{th} layers. a0, a1, a2, a3, and a4 are some of the constants to manage the learning rate of weight values.

As shown in Fig. 2, research work considered a three-layer spiking neural network. Eq.5 was used to initialize weight for layer i, j and layer j, k. Now consider i as the input layer of the network while j is considered as the hidden layer of the network. Finally, k is considered as the output layer of the network. w_{ij} represents weights of the between nodes of different consecutive layers. So the output of the layer depends on the below Eq. 6:

$$X_j = b_j + \sum x_i . w_{ij} \quad \text{Eq. 6}$$

where $1 \leq i \leq n$, n is the number of inputs x_i to node j, and bj is the biasing for node j. Sigmoid activation function was used for firing the neuron information. Desired output D was passed to check error E as in Eq. 7.Then adjusted weights get calculated by Eq. 8.

$$E = D - \text{sum}(X) \quad \text{Eq.7}$$

$$w_{ij} = w_{ij} * \Delta w \quad \text{Eq. 8}$$

Now repeat the above steps for getting output and minimizing the error values.

G. Testing of Spiking Neural Network

In this module of the proposed work, each input test image was pre-processed as done in the training module. Histogram and DWT features were also extracted from each block of the input image as done in the training module. Extracted features were normalized and passed in the trained spiking neural network to get classes of the image either infected/malignant or normal/benign.

IV. EXPERIMENT AND RESULTS

A. Dataset

Experimental values of the proposed work were obtained from three datasets taken from kaggle. Explanations of the dataset with detailed features were shown in table 2.

TABLE 2. DATASET EXPLANATION

Dataset	Features	Values
Malaria	Images	150
	Dimensions	142x163
Breast Cancer	Images	150
	Dimensions	700x460
Skin Cancer	Images	150
	Dimensions	224x224

B. Experimental discussion

Implementation of the proposed model was done on MATLAB software 2016a. A comparison of the proposed model was done with CNNMID that was proposed in [26].

a) preprocessing of image

This research considered the malaria, breast, and skin cancer images dataset for experiments. Each image converted to grayscale(range 0 to 255) also resized into a 64x64 matrix of pixels further obtained 16 blocks of size 4x4. Then block-wise histogram features were evaluated considering 8 bins; hence a single vector having 16 values of histogram features was obtained. On the other hand, image dwt2 features in size b/2xb/2 were also calculated in which approximation, horizontal, vertical, and diagonal feature components were calculated. For the processing, here considered approximation component features. For a single image, 4 values of the approximation component are considered for use. Then 16 histogram features merged with 4 values of approximation compoanent, making it a single vector of 20 values. These 20 values were then normalized, in which all positive values were set to 1, whereas 0 and negative values changed to 0. After this process, 20 valued normalized vector(N) contains only 1 and 0 values.

b) SNN training and testing

Vector N of one block of an image then passed to Spiking neural network where value 1 teated as a spike for neurons than a set of spikes for one block of an image passed to SNN at a stretch hence in this way 20-time interval was considered while processing. After processing one block of information, the neurons' value is set to zero. Then other blocks of the image are passed to SNN one by one. These spike values then get multiplied with weights decided by the presynaptic and postsynaptic communication of neurons. The sigmoid activation function decided the threshold value for passing the information from one neuron to other. From the output layer of SNN, the actual output was obtained. Calculation of error done comparing actual output with target output. Obtained errors in this way get minimized by changing of weights values. The above-summarized calculations were repeated for all blocks of an image then all images for malaria, breast cancer, and skin cancer dataset. In this way, SNN training got completed.

The testing process of SNN is used to evaluate the accuracy, precision, recall, and F- measure values.

Implementation of comparing CNNMID model was also done, which was proposed in [26].

C. Evaluation Parameters

Evaluation parameters formulas are written as follows

$$\text{Pr}\,ecision = \frac{True\_Positive}{True\_Positive + False\_Positive}$$

$$\text{Re}\,call = \frac{True\_Positive}{True\_Positive + False\_Negative}$$

$$F\_Score = \frac{2 * \text{Pr}\,ecision * \text{Re}\,call}{\text{Pr}\,ecision + \text{Re}\,call}$$

$$Accuracy = \frac{CC}{CC + IC}$$

here CC means right classification, whereas IC means the wrong classification

TABLE 3. PRECISION VALUE-BASED COMPARISON

Malaria Images	**SNMID**	**CNNMID**
25	1	0.8462
50	1	0.64
75	0.9867	0.6757
100	0.99	0.64
125	0.9921	0.6129
Breast Cancer	**SNMID**	**CNNMID**
25	0.9167	0.8462
50	0.88	0.8
75	0.78	0.7838
100	0.8733	0.78
125	0.9613	0.806
Skin Cancer	**SNMID**	**CNNMID**
25	1	0.7692
50	1	0.5909
75	1	0.5882
100	1	0.5909
125	1	0.625

D. Results

Table 3 shows that the precision value of the proposed SNMID has improved the true positive rate as compared to CNNMID. It was obtained that for different image testing dataset sizes SNMID value was always high in all sets of types of diseases. The use of image histogram features with blocked DWT features has increased the work precision value as compared to CNNMID. Fig. 3 shows precision comparing values with different testing images for all sets of diagnosis diseases.

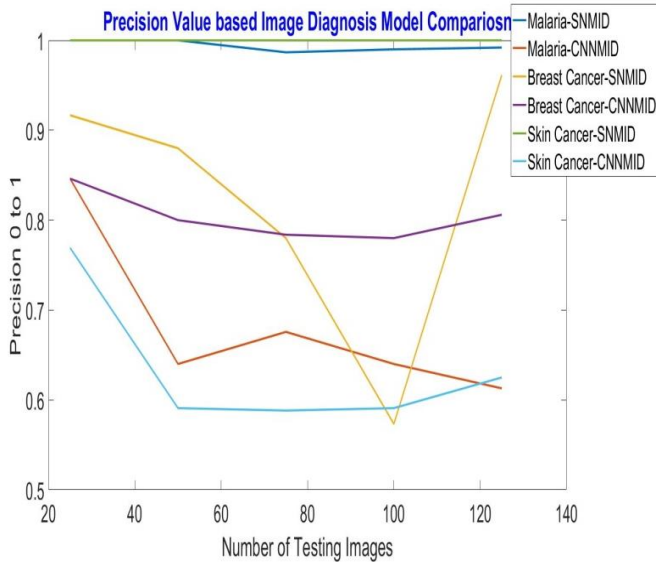

Fig: 3 Precision value vs. different testing images.

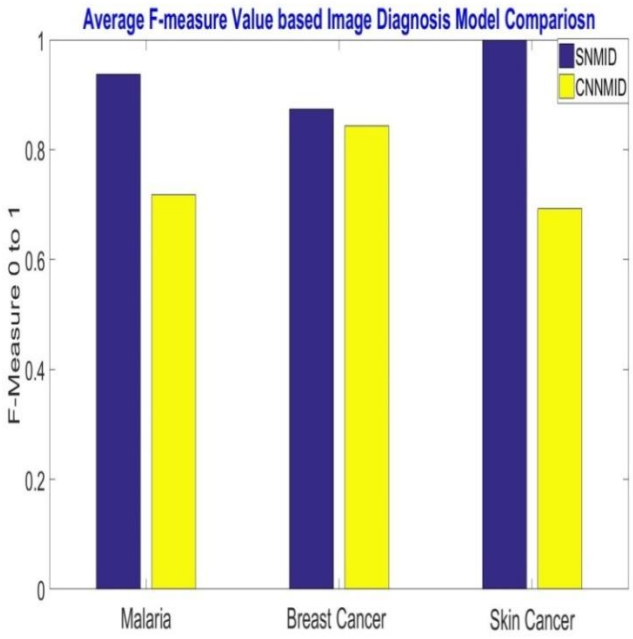

Fig. 4 Average F-measure value-based comparison

TABLE 4. RECALL VALUE-BASED COMPARISON

Malaria Images	**SNMID**	**CNNMID**
25	0.9615	1
50	0.9615	0.8421
75	0.8315	0.7576
100	0.8319	0.64
125	0.8552	0.5758
Breast Cancer	**SNMID**	**CNNMID**
25	1	1
50	0.7859	0.9524
75	0.7648	0.9063
100	0.7057	0.8298
125	0.8834	0.769
Skin Cancer	**SNMID**	**CNNMID**
25	1	0.9091
50	1	0.7647
75	1	0.8333
100	1	0.6667
125	1	0.6731

Table 4 shows recall value comparison, and table 5 shows the f-measure value-based comparison. Use of spiking neural network for learning of selected features (Histogram / DWT) in the proposed model and SNN spiking properties has improved the average recall value by 12.52 for malaria,23.06 for skin cancer; however,,, for breast cancer, CNNMID shows better performance than SNMID. The F-measure average value-based comparison also shows that SNMID performance has improved value performance by 21.87 for malaria,03.02 for breast cancer, and 30.71 for skin cancer when compared with the CNNMID model as spiking neural

networks turn the learning data into spikes for training, which directly impact the weight adjustment for triggering the neuron. Fig. 4 shows that average f-measure values were high in all cases of diagnosis diseases. Table 6 shows that the proposed model has increased the average accuracy percentage by 19.37 for malaria; for breast cancer CNNMID was superior, and for skin cancer, SNMID proved better with a 23.06 % improvement. Fig. 5 shows the accuracy vs. testing images graph in that growth can be seen for all the three diseases datasets. From the result values, it is clear that for small datasets, SNMID proved better compared to CNNMID while classification.

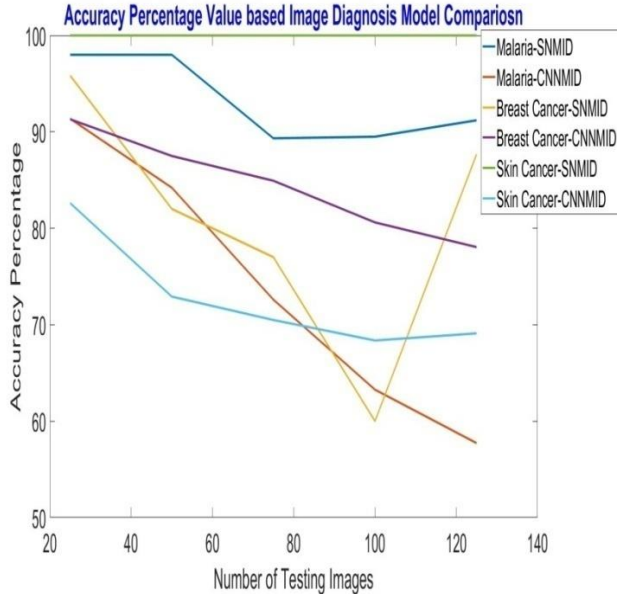

Fig. 5 Accuracy percentage value based comparison

TABLE 5. F-MEASURE VALUE BASED COMPARISON

Malaria Images	**SNMID**	**CNNMID**
25	0.9804	0.9167
50	0.9804	0.7273
75	0.9024	0.7143
100	0.9041	0.64
125	0.9185	0.5938
Breast Cancer	**SNMID**	**CNNMID**
25	0.9565	0.9167
50	0.8303	0.8696
75	0.7723	0.84
100	0.8891	0.804
125	0.9207	0.7874
Skin Cancer	**SNMID**	**Previous Model**
25	1	0.8333
50	1	0.6667
75	1	0.6897
100	1	0.6265
125	1	0.6481

TABLE 6. ACCURACY VALUE BASED COMPARISON.

Malaria Images	**SNMID**	**CNNMID**
25	97.9998	91.36
50	97.9998	84.21
75	89.3328	72.602
100	89.4996	63.2653
125	91.1997	57.7236
Breast Cancer	**SNMID**	**CNNMID**
25	95.832	91.3043
50	82.0128	87.5
75	77.006	84.9315
100	60.0031	80.612
125	87.6726	78.0488
Skin Cancer	**SNMID**	**CNNMID**
25	100	82.6087
50	100	72.9167
75	100	70.4918
100	100	68.3673
125	100	69.1057

V. CONCLUSIONS

The increased population of image-based diagnosis increases the heath load on medical experts. To reduce this load and improve the disease diagnosis level, a SNMID type computerized model can be used. Training of SNN architecture involves unsupervised learning at the initial level. Later supervised learning handles remaining calculations. This research proposed a trained and tested SNMID model for the classification of classes of malaria, breast cancer, and skin cancer datasets. Diseases features were extracted using sixteen bins histogram and second level discrete wavelet transform to get processed using SNMID. This paper included a comparison of the SNMID model with CNN based model and evaluated the conclusion that for 125 sets of images for each disease, SNMID was performing better. SNMID measured accuracy percentage was 91.20 for malaria, 87.67 for breast cancer, and 100 for skin cancer, whereas CNN measures were 57.72 for malaria, 78.05 for breast cancer, and 69.12 for skin cancer. SNMID model also performed better with regards to precision, recall, and F-measures parameters comparison with CNN model. In the future SNMID model can be trained and tested for different diseases considering big medical datasets. Researchers can also try to embed SNMID with hardware.

REFERENCES

[1] Senthilkumar, Gagan Kumar B, and Lasya K R., Artificial Intelligence Augmentation in Blood Transfusion, Biochemistry, and Hematology of Digital Pathology: A Comparative Performance Evaluation on Pathology Labs and Corporate Hospitals located in Bengaluru, International Journal of Engineering Trends and Technology, 68(12) (2020) 132-139.

[2] Muhammad Imran Razzak, Saeeda Naz, and Ahmad Zaib., Deep Learning for Medical Image Processing: Overview, Challenges and Future, Deep Learning for Medical Imaging, (2020).

[3] Geert Litjens, Thijs Kooi, Babak Ehteshami Bejnordi, Arnaud Arindra Adiyoso Setio, Francesco Ciompi, Mohsen Ghafoorian, Jeroen A.W.M.

van der Laak, Bram van Ginneken, Clara I. Sánchez., A survey on deep learning in medical image analysis, Medical Image Analysis, 42 (2017).

[4] Astha Singh, Asst. Prof. Jayshree Boaddh, Asst. Prof. Jashwant Samar., A Survey on Digital Image Retrieval Technique and Visual Features Authors, IJSRET, 7(1) 2021.

[5] Alexander Selvikvåg Lundervold, Arvid Lundervold., An overview of deep learning in medical imaging focusing on MRI, Zeitschrift für Medizinische Physik, 29(2) (2019).

[6] Mehedi Masud, Hesham Alhumyani, Sultan S. Alshamrani, Omar Cheikhrouhou, Saleh Ibrahim, Ghulam Muhammad, M. Shamim Hossain, Mohammad Shorfuzzaman., Leveraging Deep Learning Techniques for Malaria Parasite Detection Using Mobile Application, Wireless Communications and Mobile Computing, Article ID 8895429, (2020) 15.

[7] Fuhad, K.M.F.; Tuba, J.F.; Sarker, M.R.A.; Momen, S.; Mohammed, N.; Rahman, T., Deep Learning-Based Automatic Malaria Parasite Detection from Blood Smear and Its Smartphone-Based Application, Diagnostics, (2020).

[8] P. A. Pattanaik, M. Mittal and M. Z. Khan., Unsupervised Deep Learning CAD Scheme for the Detection of Malaria in Blood Smear Microscopic Images, in IEEE Access, 8 (2020) 94936-94946.

[9] Sahni P., Mittal N., Breast Cancer Detection Using Image Processing Techniques. In: Kumar M., Pandey R., Kumar V. (eds) Advances in Interdisciplinary Engineering, Lecture Notes in Mechanical Engineering. Springer, Singapore, (2019).

[10] Y. Wang., Deeply-Supervised Networks With Threshold Loss for Cancer Detection in Automated Breast Ultrasound, in IEEE Transactions on Medical Imaging, 39(4) (2020) 866-876.

[11] J. Zheng, D. Lin, Z. Gao, S. Wang, M. He, and J. Fan., Deep Learning Assisted Efficient AdaBoost Algorithm for Breast Cancer Detection and Early Diagnosis, in IEEE Access, 8 (2020) 96946-96954.

[12] Shivangi Jain, Vandana jagtap, Nitin Pise., Computer-Aided Melanoma Skin Cancer Detection Using Image Processing, Procedia Computer Science, 48 (2015).

[13] Kalwa, U.; Legner, C.; Kong, T.; Pandey, S. Skin Cancer Diagnostics with an All-Inclusive Smartphone Application, (2019). Symmetry 11, 790.

[14] Mohammad Ashraf Ottom., Convolutional Neural Network for Diagnosing Skin Cancer, International Journal of Advanced Computer Science and Applications, 10(7) (2019).

[15] Divya Srivastava, Rajesh Wadhvani, and Manasi Gyanchandani., A Review: Color Feature Extraction Methods for Content-Based Image Retrieval, IJCEM International Journal of Computational Engineering & Management, 18(3) (2015).

[16] Iqbal H. Sarker., Content-based Image Retrieval Using Haar Wavelet Transform and Color Moment, The Smart Computing Review 3(3) (2013).DOI: 10.6029/smartcr.2013.03.002.

[17] Naoya Muramatsu and Hai-Tao Yu., Combining SNN and ANN for enhanced image classification, Neural and Evolutionary Computing, arXiV.org:2102.10592, (2021).

[18] Taeyoon Kim et al., Spiking Neural Network (SNN) With Memristor Synapses Having Non-linear Weight Update, Frontiers in Computational science, (2021). https://doi.org/10.3389/fncom.2021.646125

[19] Schliebs, S; Kasabov, N., Evolving spiking neural networks: A Survey, Zurich Open Repository and Archive , Zurich Open Repository and Archive, (2013).

[20] S. G. Wysoski, L. Benuskova, and N. Kasabov., Fast and adaptive network of spiking neurons for multi-view visual pattern recognition, Neurocomputing, 71(13) (2008) 2563–2575.

[21] Taki Hasan Rafi., A Brief Review on Spiking Neural Network - A Biological Inspiration, preprints.org, doi: 10.20944/preprints202104.0202.v1, Online: 7 April 2021

[22] Vijayalakshmi, D., Nath, M.K. & Acharya, O.P., A Comprehensive Survey on Image Contrast Enhancement Techniques in Spatial Domain. Sens Imaging, 21(40) (2020).

[23] Varun Srivastava, Ravindra Kumar Purwar., A Five-Level Wavelet Decomposition and Dimensional Reduction Approach for Feature Extraction and Classification of MR and CT Scan Images, Applied Computational Intelligence and Soft Computing, Article ID 9571262, 9 (2017).

[24] AmirhosseinTavanaei, Anthony S. Maida., A Minimal Spiking Neural Network to Rapidly Train and Classify Handwritten Digits in Binary and 10-Digit Tasks, (IJARAI) International Journal of Advanced Research in Artificial Intelligence, 4(7) (2015).

[25] Pritam Bose, Nikola K. Kasabov, Lorenzo Bruzzone, and Reggio N. Hartono., Spiking Neural Networks for Crop Yield Estimation Based on Spatiotemporal Analysis of Image Time Series, IEEE transactions on geoscience and remote sensing, (2016).

[26] Quan Quan, Jianxin Wang, Liangliang Liu., An Effective Convolutional Neural Network for Classifying Red Blood Cells in Malaria Diseases, Interdisciplinary Sciences: Computational Life Sciences, (2020).